# Benchmark problems for predictive fem simulation of 1-D and 2-D guided waves for structural health monitoring with piezoelectric wafer active sensors

M. Gresil, Y. Shen, and V. Giurgiutiu

Citation: AIP Conference Proceedings **1430**, 1835 (2012); doi: 10.1063/1.4716434
View online: http://dx.doi.org/10.1063/1.4716434
View Table of Contents: http://scitation.aip.org/content/aip/proceeding/aipcp/1430?ver=pdfcov
Published by the AIP Publishing

**Articles you may be interested in**

Ultrasonic wave-based structural health monitoring embedded instrument
Rev. Sci. Instrum. **84**, 125106 (2013); 10.1063/1.4834175

Lamb wave structural health monitoring using frequency-wavenumber analysis
AIP Conf. Proc. **1511**, 302 (2013); 10.1063/1.4789062

High performance wireless sensors system for structural health monitoring
AIP Conf. Proc. **1430**, 1583 (2012); 10.1063/1.4716403

Application of Mellin transform features for robust ultrasonic guided wave structural health monitoring
AIP Conf. Proc. **1430**, 1551 (2012); 10.1063/1.4716399

A Wireless Ultrasonic Guided Wave Structural Health Monitoring System for Aircraft Wing Inspection
AIP Conf. Proc. **894**, 1548 (2007); 10.1063/1.2718149

Reuse of AIP Publishing content is subject to the terms at: https://publishing.aip.org/authors/rights-and-permissions IP: 141.212.190.175 On: Fri, 15 Apr 2016 19:10:28

# BENCHMARK PROBLEMS FOR PREDICTIVE FEM SIMULATION OF 1-D AND 2-D GUIDED WAVES FOR STRUCTURAL HEALTH MONITORING WITH PIEZOELECTRIC WAFER ACTIVE SENSORS

M. Gresil, Y. Shen, and V. Giurgiutiu

Laboratory for Active and Smart Structures, Department of Mechanical Engineering, University of South Carolina, Columbia, SC 29208

**ABSTRACT.** Predictive simulation of ultrasonic nondestructive evaluation and structural health monitoring (SHM) is challenging. This paper addresses this issue in the context of guided-waves with piezoelectric wafer active sensors (PWAS). The principle of guided wave with PWAS transducers is studied and an analytical model is developed to predict the waveform and theoretical frequency contents solution. Two benchmark problems, one 1-D and the other 2-D to achieve reliable and trustworthy predictive simulation of guided wave with finite element method have also been proposed.

**Keywords:** Guided Waves, Finite Element Method, Piezoelectric, Structural Health Monitoring
**PACS:** 80

## INTRODUCTION

Predictive simulation of ultrasonic non-destructive evaluation (NDE) and structural health monitoring (SHM) in realistic structures is challenging [1]. Analytical methods (e.g., ray-tracing, beam/pencil, Green functions, etc.) [2] that can efficiently model wave propagation are limited to simple geometries. Realistic structures with complicated geometries are usually modeled with the finite element method (FEM). Commercial FEM codes offer convenient built-in resources for automated meshing, frequency analysis, and time integration of dynamic events. Even a relatively rough FE model would yield a 'wave propagation' animation that is illustrative and interesting to watch. However, obtaining accurate wave propagation solutions at ultrasonic frequencies is computationally intensive and may become prohibitive for realistic structures. Several investigators have previously addressed the convergence of FEM solutions for NDE-type ultrasonic inspection (bulk waves) and have developed useful guidelines [3, 4]. This paper addresses this issue in the context of guided-waves for SHM with piezoelectric wafer active sensors (PWAS) using the pitch-catch method.

*Review of Progress in Quantitative Nondestructive Evaluation*
AIP Conf. Proc. 1430, 1835-1842 (2012); doi: 10.1063/1.4716434
© 2012 American Institute of Physics 978-0-7354-1013-8/$30.00



Reuse of AIP Publishing content is subject to the terms at: https://publishing.aip.org/authors/rights-and-permissions IP: 141.212.190.175 On: Fri, 15 Apr 2016 19:10:28

## ANALYTICAL MODELING

The analytical modeling of the pitch-catch process between two PWAS transducers separated by a distance $x$ was carried out in the frequency domain in four steps: (i) Fourier transform the time-domain excitation signal $V_e(t)$ taken into the frequency domain spectrum, $\tilde{V}_e(\omega)$; (ii) calculate the frequency-domain structural transfer function at the receiver location, $G(x,\omega)$; (iii) multiply the structural transfer function by frequency-domain excitation signal to obtain the frequency domain signal at the receiver, i.e., $\tilde{V}_r(x,\omega) = G(x,\omega)\cdot\tilde{V}_e(\omega)$; (iv) perform inverse Fourier transform to obtain the time-domain receiver signal $V_r(x,t) = IFFT\{\tilde{V}_r(x,\omega)\} = IFFT\{G(x,\omega)\cdot\tilde{V}_e(\omega)\}$. The structural transfer function $G(x,\omega)$ is given by Eq. (99) of ref.[1], page 327, which gives the in-plane strain at the plate surface as

$$\varepsilon_x(x,t) = -i\frac{a\tau_0}{\mu}\left\{\sum_{\xi^S}(\sin\xi^S a)\frac{N_S(\xi^S)}{D_S'(\xi^S)}e^{-i\left(\xi^S x-\omega t\right)} + \sum_{\xi^A}(\sin\xi^A a)\frac{N_A(\xi^A)}{D_A'(\xi^A)}e^{-i\left(\xi^A x-\omega t\right)}\right\} \tag{1}$$

where $\xi$ is the frequency dependent wave number of each Lamb wave mode and the superscripts *S* and *A* refer to symmetric and antisymmetric Lamb wave modes. The notations of ref.[1], pages 321-329 are adopted. If only the two fundamental modes, S0 and A0, are present, then $G(\omega)$ can be written as

$$G(x,\omega) = S(\omega)e^{-i\xi^S x} + A(\omega)e^{-i\xi^A x} \tag{2}$$

$$S(\omega) = \kappa_{PWAS}\ \sin\xi^S a\ \frac{N_S(\xi^S)}{D_S'(\xi^S)} \qquad A(\omega) = \kappa_{PWAS}\ \sin\xi^A a\ \frac{N_A(\xi^A)}{D_A'(\xi^A)} \tag{3}$$

where $\kappa_{PWAS}$ is the complex transduction coefficient that converts applied strain into PWAS voltage. The modal participation functions $S(\omega)$ and $A(\omega)$ determine the amplitude of the S0 and A0 wave modes excited into the structure. The terms $\sin(\xi^S a)$ and $\sin(\xi^A a)$ control the tuning effect between the PWAS transducer and the Lamb waves. Hence, the signal at the receive PWAS is

$$V_r(x,\omega) = S(\omega)\tilde{V}_e(\omega)e^{-i\xi^S x} + A(\omega)\tilde{V}_e(\omega)e^{-i\xi^A x} \tag{4}$$

## 1-D FEM MODELING

In the context of wave propagation modeling with the finite element method (FEM), the choice of the solver technique, mesh density, and time step influences the successful wave simulation and the level of accuracy with which the physical phenomenon is represented. For time domain models solved with an explicit solver, we investigated the influence of the mesh density for linear quadrilateral elements for both A0 and S0 modes waves using the commercial software ABAQUS. Both S0 and A0 waves are considered; they are excited by a pair of two self-equilibrating nodal forces. The distance between the two forces corresponds to the real size of the PWAS. The time domain excitation signal considered in our studies consisted of a 150


Reuse of AIP Publishing content is subject to the terms at: https://publishing.aip.org/authors/rights-and-permissions IP: 141.212.190.175 On: Fri, 15 Apr 2016 19:10:28

kHz three-count tone burst filtered through a Hanning window. The distance between the transducer and the receiver was 100 mm. Figure 1a highlights the influence of the mesh density on the group velocity error: it is very strong for the A0 mode compared to the S0 mode where we obtain a good accuracy for a lower mesh density. The mesh density is expressed as $N = \lambda / L$ elements per wavelength, where λ is the wavelength and L is the element size. The curve shows how the A0 error varies from a value of about 9% for N=15 to a value of 0.2% for N=254. The S0 error varies from a value of about 2% for N=20 to a value of 0.15% for N=120. The mesh density has a great impact on the computational model size and therefore the amount of time and memory required for solving the problem. Figure 1b shows the calculation time for the explicit and implicit solvers in ABAQUS versus mesh density N. The explicit solver is much more efficient than the implicit solver even for a low mesh density.

## VALIDATION

The analytical predictions and the FEM results were compared with experimental data for a 1-mm thick aluminum plate with two PWAS at 100-mm distance and a frequency of 150 kHz (Fig. 2a). The S0 and A0 wave packets are observed. The group velocity of S0 mode is higher than the A0 mode, so the S0 wave packet is picked up earlier than the A0 wave packet. Since the excitation signal has a center frequency of 150 kHz, we would have thought that the center frequencies of the A0 and S0 packets would also be 150 kHz. In fact, as shown in Fig. 2b, this is not the case. We note that the center frequency of the A0 mode underwent a shift towards lower frequencies while the S0 mode underwent a shift towards higher frequencies.

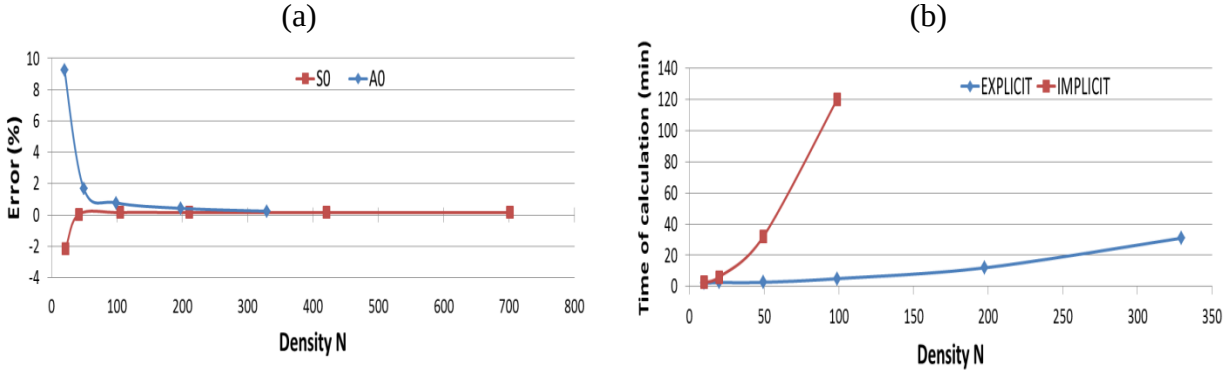


**FIGURE 1.** (a) Group velocity versus the mesh density for the S0 and A0 mode; (b) Time of calculation for the explicit or implicit solver versus the mesh density N.

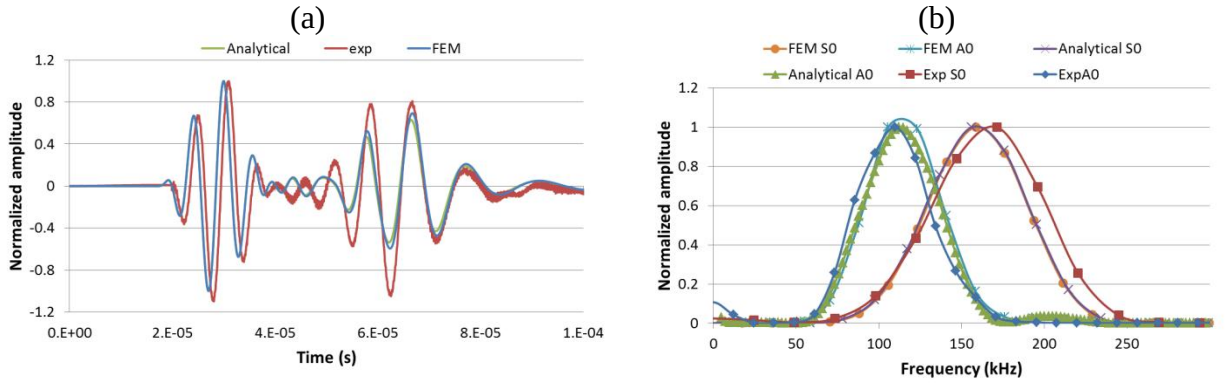


**FIGURE 2.** (a) Comparison between the analytical, FEM and experimental receive signal from the PWAS for a 150 kHz frequency; (b) FFT of the S0 and A0 wave packet for the analytical, FEM and experimental signal received.


Reuse of AIP Publishing content is subject to the terms at: https://publishing.aip.org/authors/rights-and-permissions IP: 141.212.190.175 On: Fri, 15 Apr 2016 19:10:28

A theoretical solution for this numerically observed phenomenon is as follows; the magnitudes of frequency contents for S0 and A0 are

$$\left|V_{Sr}(\omega)\right| = \left|\left(\sin k^S a\right)\frac{N_S\left(k^S\right)}{D_S'\left(k^S\right)}\right| \qquad \left|V_{Ar}(\omega)\right| = \left|\left(\sin k^A a\right)\frac{N_A\left(k^A\right)}{D_A'\left(k^A\right)}\right| \bullet \left|V_e(\omega)\right| \tag{5}$$

Hence, the amplification coefficients for each package are

$$C_S = \left|\left(\sin k^S a\right)\frac{N_S\left(k^S\right)}{D_S'\left(k^S\right)}\right| \qquad C_A = \left|\left(\sin k^A a\right)\frac{N_A\left(k^A\right)}{D_A'\left(k^A\right)}\right| \tag{6}$$

The amplification coefficients are directly related to the PWAS size *a*, material properties, plate thickness, and the excitation frequency. A numerical representation of this theoretical solution is shown in Fig. 3 for a 150 kHz Hanning-window modulated tone burst excitation signal and a 7-mm PWAS transducer on a 1-mm thick aluminum plate. Figure 3 shows the frequency contents of A0 and S0 pitch-catch signals. At this frequency, we notice that A0 shifted toward lower frequencies and S0 toward higher frequencies as observed experimentally and in FEM simulation thus clarifying this intriguing phenomenon. These results apply for a PWAS of finite size. If the excitation is done by a single point force, or if the PWAS becomes vanishingly small, $a \to 0$, then the frequency shifts do not happen.

## SOFTWARE DEVELOPMENT

The software program 'WaveFormRevealer' has been developed in Matlab graphical user interface (GUI) environment to predict the waveform of the analytical modeling. The GUI of the software is shown in Fig. 4.

This software allows users to get the desired analytical solution by inputting material properties, specimen geometry, excitation signal count number, excitation signal frequency, and time range. It can also show a continuous waveform change by clicking on the frequency control slider, which is just like the waveform shown on an oscilloscope when adjusting the excitation signal frequency. The time range to show a waveform could also be set by users through entering the 'Range' information. Analytical waveforms could also be stored in Excel files by a click on the 'SAVE' button.

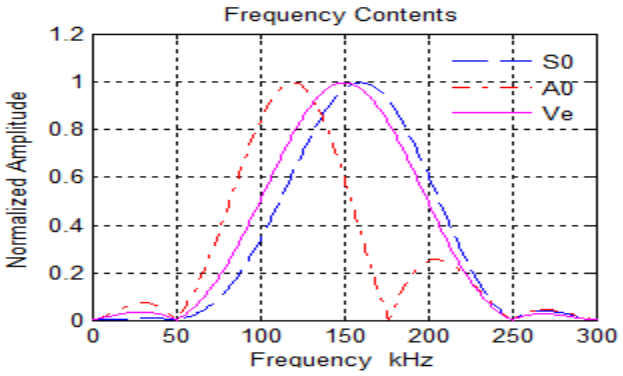


**FIGURE 3.** Frequency contents of S0 and A0 packets and excitation Ve at 150 kHz.


Reuse of AIP Publishing content is subject to the terms at: https://publishing.aip.org/authors/rights-and-permissions IP: 141.212.190.175 On: Fri, 15 Apr 2016 19:10:28

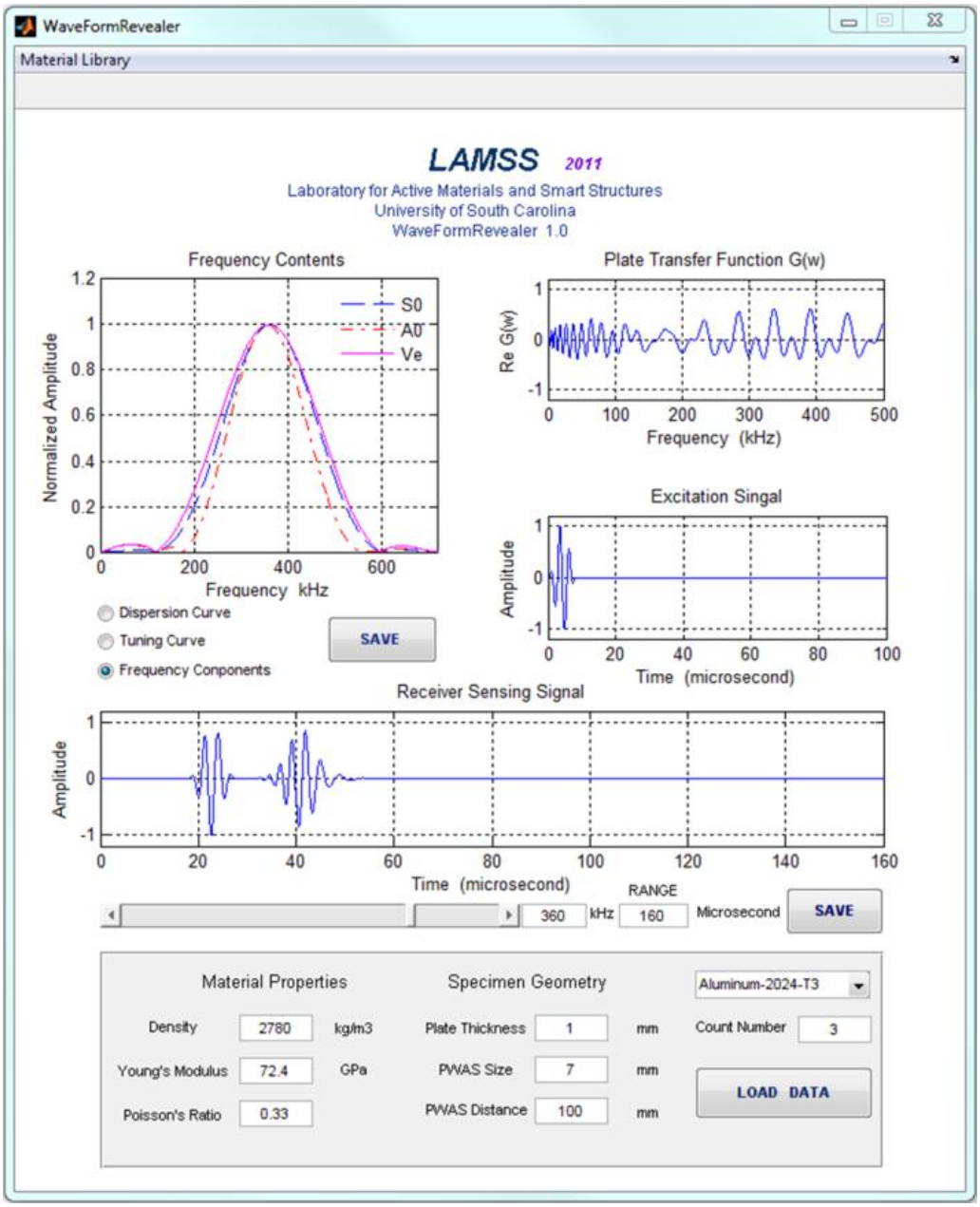


**FIGURE 4.** Graphical User Interface (GUI) of the "WaveFormRevealer".

## 2-D FEM MODELING

The use of finite element method to model the generation of elastic waves from a simulated PWAS excitation in a 2D plate has been explored. We modeled the guided wave generation and reception in a rectangular 12-mm thick steel plate containing a through-hole defect (Fig. 5a).

We used the ABAQUS/explicit solver because it gives a better trade-off between accuracy and computation time. The piezoelectric element doesn't exist in ABAQUS/explicit; hence we applied 12 self-equilibrating forces as shown in Fig. 5b to simulate the wave excitation. A 3-count smoothed tone burst with a central frequency of 141 kHz was used to modulate the excitation. (This frequency corresponds at the best experimental damage detection configuration for this type of defect). The excitation was applied to PWAS P0 and received by PWAS P4 (Fig. 5). The wave reception was done by monitoring the radially resolved surface


Reuse of AIP Publishing content is subject to the terms at: https://publishing.aip.org/authors/rights-and-permissions IP: 141.212.190.175 On: Fri, 15 Apr 2016 19:10:28

strain $\varepsilon_r$ at the center of the receiver PWAS. Figure 6 shows the analytical and FEM simulations compared with experimental measurement at PWAS P4. The first wave packet corresponds to the S0 mode. A very good agreement is observed between the experimental and the FEM results. The analytical solution is not as good; this may be due to the fact that the analytical model is only a 1D model. The second wave packet corresponds to the A0 mode. Here, we observe a very good agreement between the analytical results and the FEM results. But we observe a time shift between these two results and the experimental result. This may due to the fact that we used a circular PWAS in the experimental tests but a square PWAS in FEM simulation.

The signal predicted on the pristine plate is compared with the signal modified by the presence of a 7.9 mm through hole placed between transmitter and receiver. The results using the FEM approach are given in Fig. 7a and the experimental results are given in Fig. 7b. The hole effect in the signal consists of little phase shifts and amplitude decreases.

In order to have an SHM system able to evaluate in real time, in situ, the health of the structure in an automatic way, it is necessary to define a damage index (DI). We chose the DI defined by Zhao et al. [5] which gives very reproducible results and is easy to implement.

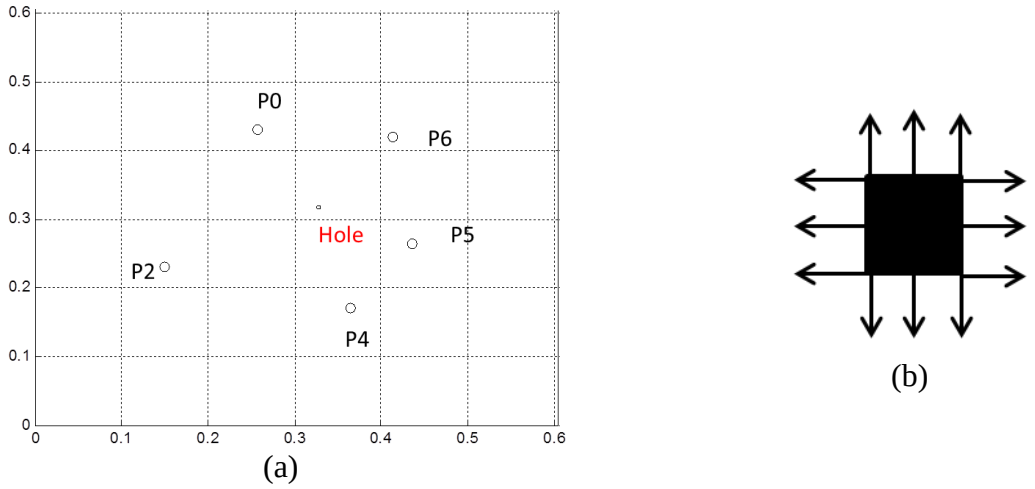


**FIGURE 5.** (a) FEM and experimental configuration; (b) self-equilibrated forces applied to simulate the displacement occur by the PWAS P0.

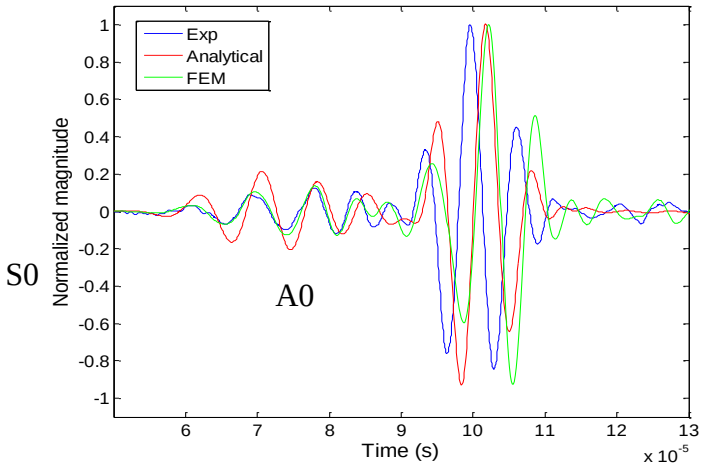


**FIGURE 6.** Experimental, Analytical and FEM receive signal by the PWAS P4 in the pristine case.



Reuse of AIP Publishing content is subject to the terms at: https://publishing.aip.org/authors/rights-and-permissions IP: 141.212.190.175 On: Fri, 15 Apr 2016 19:10:28

$$DI = 1 - \rho, \qquad \rho = \frac{C_{XY}}{\sigma_X \sigma_Y} \tag{7}$$

where $\rho$ is the correlation coefficient between two signals and

$$C_{XY} = \sum_{k=1}^{K} \left(X_k - \mu_x\right)\left(Y_k - \mu_y\right), \qquad \sigma_X \sigma_Y = \sqrt{\sum_{k=1}^{K} \left(X_k - \mu_x\right)^2 \left(Y_k - \mu_y\right)^2} \tag{8}$$

where $X$ is the reference data set (baseline) and $Y$ is the new data set recorded after a period of service time $C_{XY}$ is the covariance of $X$ and $Y$; $\mu$ is the mean of the respective data set; $K$ is the length of the data set; and $\sigma_X$ and $\sigma_Y$ are the standard deviations of $x$ and $y$, respectively.

This DI was used to detect the hole defect and track its growth in order to compare the experimental and the FEM results. The DI was calculated for different stages of the defect growth. Figure 8 shows the DI as the diameter of the hole increased from 2 mm through, 4, 6, 7.9 and 9.8 mm. The DI increased with the increase in the defect severity. A very similar slope of the curve is observed between the FEM approach and the experimental results.

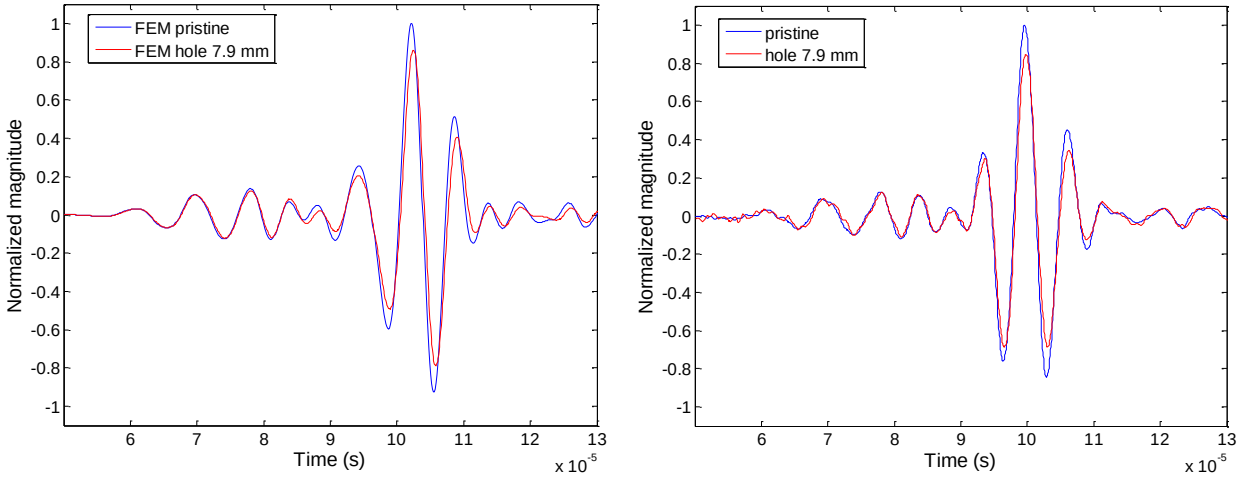


(a) (b)

**FIGURE 7.** Comparison between the pristine and the defect signal with a hole of 7.9 mm (a) for the FEM approach and (b) for the experimental results.

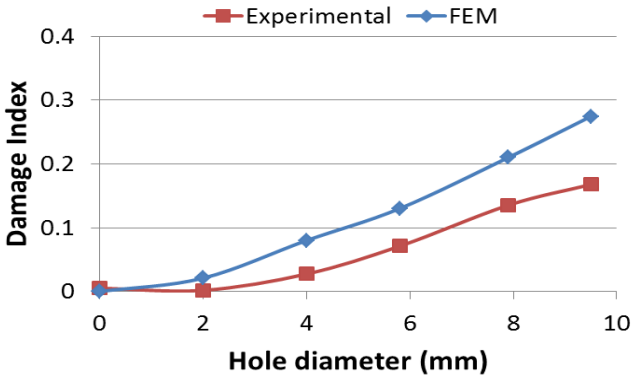


**FIGURE 8.** Comparison of the damage index based on the correlation coefficient between the experimental and the FEM.



Reuse of AIP Publishing content is subject to the terms at: https://publishing.aip.org/authors/rights-and-permissions IP: 141.212.190.175 On: Fri, 15 Apr 2016 19:10:28

## CONCLUSION

Theory of guided wave propagation between two PWAS transducers was studied and analytical model was built to give the theoretical waveforms and the frequency contents of pitch-catch signals. Analytical modeling and finite element modeling have good match with experimental results, and can well describe guided wave propagation between two PWAS transducers. A theoretical explanation for frequency shift in pitch-catch signal is put forward and the theoretical solution matches well with FEM result and experimental data. The experimental frequency shift direction and size are well predicted by the theoretical solution for S0 wave package and FEM result for A0 package. The analytical model is expected to be extended to 3D circular PWAS analysis, and the Bessel function will be studied and included in future work to realize guided wave propagation between two circular PWAS transducers.

For further study, the analytical modeling is expected to include damage in the plate structure using a non-linearity aspect. The analytical modeling is expected to include damage/flaws in the plate structure, more complex structure (plate with double stiffener), and also include the second mode A1 and S1.

## ACKNOWLEDGEMENTS

This work was supported by the Office of Naval Research grant #N00014-11-1-0271, Program Director Dr. Ignacio Perez and U.S. department of commerce, National Institute of Standards and Technology (NIST), cooperative agreement number #70NANB9H9007.

## REFERENCES

1. Giurgiutiu, V., *Structural Health monitoring with piezoelectric wafer active sensor*, Elsevier Inc., 2008.
2. Fromme, P. and Sayir, M.B., "Detection of cracks at rivet holes using guided waves", *Ultrasonics*, 2002. 40(1-8): p. 199-203.
3. Drodz, M.B., "Efficient finite element modeling of ultrasound waves in elastic media", 2008, Imperial College of London: London.
4. Rajagopal, P., Drozdz, M., and Lowe, M. J. S., “Towards Improved Finite Element Modelling of the Interaction of Elastic Waves with Complex Defect Geometries”, in Review of Progress in QNDE,28A, edited by D. O. Thompson and D. E. Chimenti, AIP Conference Proceedings vol. 1096(1), American Institute of Physics, Melville, NY (2009), pp. 49-56.
5. Zhao, X., et al., "Active health monitoring of an aircraft wing with embedded piezoelectric sensor/actuator network: I. Defect detection, localization and growth monitoring", *Smart materials and structures*, 2007. 16(4): p. 1208-1217.



Reuse of AIP Publishing content is subject to the terms at: https://publishing.aip.org/authors/rights-and-permissions IP: 141.212.190.175 On: Fri, 15 Apr 2016 19:10:28